

**Methyl and Silyl Mesolytic Dissociations in the Radical Cations and Radical Anions of But-1-ene, Allylsilane, Hexa-1,3-diene, and Penta-2,4-dienylsilane. CAS–MCSCF and Coupled Cluster Theoretical Study**

Claudio Carra,<sup>†</sup> Giovanni Ghigo, and Glauco Tonachini\*

*Dipartimento di Chimica Generale ed Organica Applicata, Università di Torino, Corso Massimo D'Azeglio 48, 10125 Torino, Italy*

*claudio@photo.chem.uottawa.ca; giovanni.ghigo@unito.it; glauco.tonachini@unito.it*

*Received March 20, 2003*

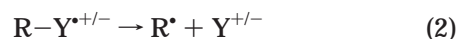
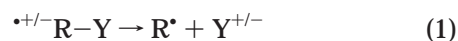
Methyl or silyl dissociation in the  $\text{CH}_2=\text{CHCH}_2\text{-XH}_3$  ( $\text{a-XH}_3^{+\cdot}$ ) and  $\text{CH}_2=\text{CHCH}=\text{CHCH}_2\text{-XH}_3$  ( $\text{p-XH}_3^{+\cdot}$ ) radical cations ( $\text{X} = \text{C}, \text{Si}$ ) yields  $\text{a}^+$  or  $\text{p}^+$  and  $\text{XH}_3^\cdot$ . Similarly, the radical anions  $\text{a-CH}_3^{\cdot-}$  and  $\text{p-CH}_3^{\cdot-}$  give the  $\pi$ -delocalized anion and  $\text{CH}_3^\cdot$  preferentially. In contrast,  $\text{a-SiH}_3^{\cdot-}$  and  $\text{p-SiH}_3^{\cdot-}$  prefer to dissociate into the  $\pi$ -delocalized radical and silide. All reactions are endoergic: by 43–50 kcal mol<sup>-1</sup> in the radical cations, and easier to some extent in the radical anions, that require 29–33 ( $\text{X} = \text{C}$ ) and 13–14 kcal mol<sup>-1</sup> ( $\text{X} = \text{Si}$ ). The fragmentation energy profiles do not present significant barriers for the backward process in the case of the radical cations. All radical anions exhibit an energy maximum along the dissociation pathway, but the barrier is lower than the dissociation limit. Fragmentation is “activated” more in the anions than in the cations with respect to homolysis in the corresponding neutrals (that requires 72–81 kcal mol<sup>-1</sup>). Wave function analysis indicates that the C–X bond cleavage in the hydrocarbon radical ions, although formally comparable to a homolytic process, is at variance with this model, due to the spin recoupling of one of the two C–X bond electrons with the originally unpaired electron. This is basically true also for the silyl-substituted radical anions, in which the initial more delocalized charge distribution might suggest some heterolytic character of the bond cleavage.

**Introduction**

Organic radical cations and radical anions were obtained in the last years from neutral precursors by different means, including photoionization,<sup>1</sup> photoinduced electron transfer,<sup>2</sup> electrochemical<sup>3–5</sup> or pulse-radiolytic<sup>6</sup> methods, and ionization by electron ionization.<sup>7</sup> Species of this kind have been observed oftentimes to undergo fragmentation into one free radical and one charged species. Fragmentation can be of synthetic interest,<sup>1</sup> and also has been exploited as a mechanistic probe for electron transfer in organic and biological reactions.<sup>8</sup>

Radical ions have either one electron less or one electron more than some precursor neutral molecule, and

are often found to undergo easier fragmentation than the neutrals.<sup>9,10</sup> Within a localized picture, the breaking  $\sigma$  bond can be supposed to be weakened, and activated toward cleavage, by loss or gain of one electron. Some formal criteria about the charge and spin partitioning as the radical ion  $\text{R-Y}$  dissociates have been used, classifying the process as heterolysis when the charge, localized on R, moves to Y as the bond cleaves (with “regioconservation” of the spin density, eq 1), and homolysis if the charge is left where it was already localized (eq 2).<sup>10</sup>



Maslak and Narvaez originally stated:<sup>10a</sup> “the fragmentation of ... radical ions leads to radicals and ions in a process that may be viewed as homolytic or heterolytic

<sup>†</sup> Present address: Department of Chemistry, University of Ottawa, 10 Marie Curie, Ottawa, Canada K1N 6N5.

(1) Lew, C. S. Q.; Brisson, J. R.; Johnston, L. J. *J. Org. Chem.* **1997**, *62*, 4047–4056.

(2) Albin, A.; Mella, M.; Freccero, M. *Tetrahedron* **1994**, *50*, 575–607 (Tetrahedron Report no. 348) and references therein.

(3) Zheng, Z.-R.; Evans, D. H.; Chan-Shing, E. S.; Lessard, J. *J. Am. Chem. Soc.* **1999**, *121*, 9429–9434.

(4) Andersen, M. L.; Mathivanan, N.; Wayner, D. D. M. *J. Am. Chem. Soc.* **1996**, *118*, 4871–4879.

(5) (a) Andrieux, C. P.; Savéant, J.-M.; Tallec, A.; Tardivel, R.; Tardy, C. *J. Am. Chem. Soc.* **1997**, *119*, 2420–2429. (b) Constantin, C.; Hapiot, P.; Médebielle, M.; Savéant, J.-M. *J. Am. Chem. Soc.* **1999**, *121*, 4451–4460.

(6) Closs, G. L.; Calcaterra, L. T.; Green, N. J.; Penfield, K. W.; Miller, J. R. *J. Phys. Chem.* **1986**, *90*, 3673–3683. Meot-Ner, N.; Neta, P.; Norris, R. K.; Wilson, K. *J. Phys. Chem.* **1986**, *90*, 168–173.

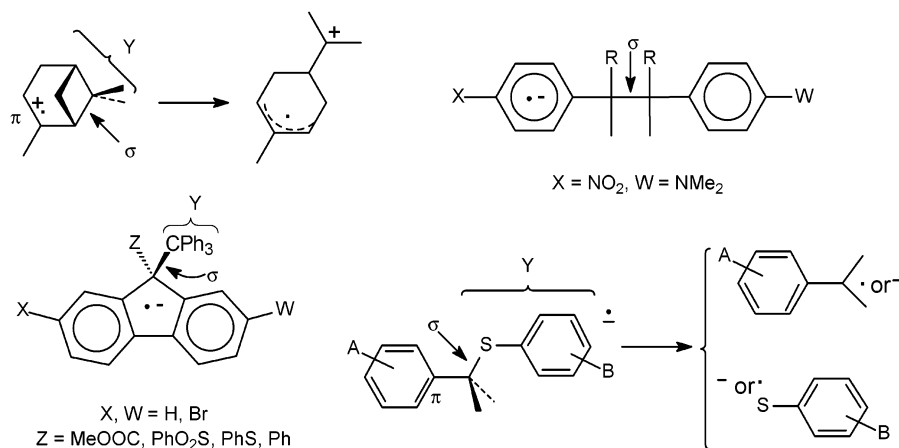
(7) Chiavarino, B.; Crestoni, M. E.; Fornarini, S. *Organometallics* **2000**, *19*, 844–848.

(8) Tanner, D. D.; Chen, J. J.; Chen, L.; Luelo, C. *J. Am. Chem. Soc.* **1991**, *113*, 8074–8081. Tanner, D. D.; Stein, A. R. *J. Org. Chem.* **1988**, *53*, 1642–1646. Tanko, J. M.; Brammer, L. E.; Hervas, M.; Campos, K. *J. Chem. Soc., Perkin Trans. 2* **1994**, 1407–1409.

(9) Chanon, M.; Rajzmann, M.; Chanon, F. *Tetrahedron* **1990**, *46*, 6193–6299 (Tetrahedron Report no. 280) and references therein.

(10) (a) Maslak, P.; Narvaez, J. N. *Angew. Chem., Int. Ed. Engl.* **1990**, *29*, 283–285. (b) Maslak, P.; Vallombroso, T. M.; Chapman, W. H., Jr.; Narvaez, J. N. *Angew. Chem., Int. Ed. Engl.* **1994**, *33*, 73–75. (c) Maslak, P.; Theroff, J. *J. Am. Chem. Soc.* **1996**, *118*, 7235–7236 and references therein.

## SCHEME 1

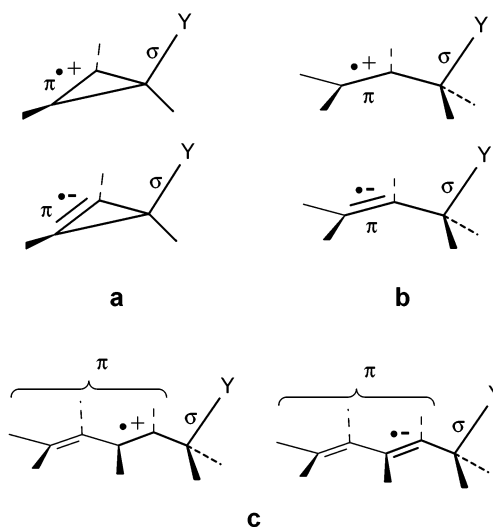


depending on electron apportionment to the fragments. To reflect this mechanistic duality we propose to call such processes mesolytic<sup>27</sup>. As will be discussed below, some ambiguities that arise from the initial electron density distribution and the spin recoupling pattern related to the bond cleavage also suggest not to use the words homolysis and heterolysis for these fragmentations, and might further justify the use of the word *mesolysis*.

A few examples of radical ion fragmentations (Scheme 1) serve to illustrate how the systems studied experimentally<sup>11–21</sup> are commonly composed of a  $\pi$  subsystem (R),  $\beta$  to the  $\sigma$  bond involved in the fragmentation (arrow). The  $\sigma$  bond connects another part of the molecule, Y, which can be saturated as well as unsaturated.

Cleavage processes in organic radical ions have been examined in some *ab initio*<sup>22</sup> and semiempirical<sup>23–26</sup> theoretical studies, while other papers have dealt with this subject from both an experimental and a theoretical point of view.<sup>27,28</sup> In the first study carried out in this laboratory, the nature of the C–C or C–Si  $\sigma$  bond

## SCHEME 2



cleavage process, which follows the generation of a radical cation or anion from neutral model precursors, was examined.<sup>29</sup> Four rigid and symmetric ( $C_3$ ) methyl or silyl-cyclopropenyl model radical cations and anions were studied (Scheme 2a, Y = CH<sub>3</sub> or SiH<sub>3</sub>). The present study concerns the gas-phase fragmentations of C<sub>1</sub> open-chain systems: four radical cations, four radical anions, and four corresponding neutrals. The smaller systems (Scheme 2b) are related, as regards structure and bonding, to the Scheme 2a radical ions. In the radical ions shown in Scheme 2c the  $\pi$  system is extended to a dienyl component. In the Scheme 2b and 2c radical ions (and their neutrals), the dissociations produce methyl or silyl (Y) and allyl or pentadienyl (R) moieties.

## Methods

The study of the model reactions discussed below was performed by determining, on the reaction energy hypersurfaces, the critical points corresponding to stable and transition structures. These were fully optimized by using gradient optimization procedures<sup>30</sup> at the CAS-MCSCF level of theory,<sup>31</sup> with the polarized split-valence shell 6-31G(d)<sup>32a,b</sup> basis set. This theory level is expected to take into account a large share

(11) d'Alessandro, N.; Albin, A.; Mariano, P. S. *J. Org. Chem.* **1993**, *58*, 937–942.

(12) Baciocchi, E.; Bernini, R.; Lanzalunga, O. *J. Chem. Soc., Chem. Commun.* **1993**, 1691–1692.

(13) Arnett, E. M.; Venimadhavan, S. *J. Am. Chem. Soc.* **1991**, *113*, 6967–6975.

(14) Venimadhavan, S.; Amarnath, K.; Harvey, N. G.; Cheng, J.-P.; Arnett, E. M. *J. Am. Chem. Soc.* **1992**, *114*, 221–229.

(15) Zhang, X.-M.; Bordwell, F. G. *J. Am. Chem. Soc.* **1992**, *114*, 9787–9792.

(16) Zhang, X.-M.; Bordwell, F. G.; Bares, J. E.; Cheng, J.-P.; Petrie, B. C. *J. Org. Chem.* **1993**, *58*, 3051–3059.

(17) Zhang, X.-M. *J. Chem. Soc., Perkin Trans. 2* **1993**, 2275–2279.

(18) Zhang, X.-M.; Bordwell, F. G. *J. Am. Chem. Soc.* **1994**, *116*, 904–908.

(19) Ichinose; Mizuno; Otsuji; Tachikawa *Tetrahedron Lett* **1994**, *35*, 587–590.

(20) Popielarz, R.; Arnold, D. R.; Du, X. *J. Am. Chem. Soc.* **1990**, *112*, 3068–3082.

(21) Arnold, D. R.; Du, X. *J. Am. Chem. Soc.* **1989**, *111*, 7666–7667.

(22) Du, X.; Arnold, D. R.; Boyd, R. J.; Shi, Z. *Can. J. Chem.* **1991**, *69*, 1365–1375.

(23) Villar, H.; Castro, E. A.; Rossi, R. A. *Can. J. Chem.* **1982**, *60*, 2525–2527.

(24) Takahashi, O.; Kikuchi, O. *Tetrahedron Lett.* **1991**, *32*, 4933–4936.

(25) Takahashi, O.; Morihashi, K.; Kikuchi, O. *Tetrahedron Lett.* **1990**, *31*, 5175–5178.

(26) Camaioni *J. Am. Chem. Soc.* **1990**, *112*, 9475–9483.

(27) Bouchoux, G.; Alcaraz, C.; Dutuit, O.; Nguyen, M. T. *J. Am. Chem. Soc.* **1998**, *120*, 152–160.

(28) Herberth, T.; Roth, H. D. *J. Am. Chem. Soc.* **1998**, *120*, 11904–11911.

(29) Carra, C.; Fiussello, F.; Tonachini, G. *J. Org. Chem.* **1999**, *64*, 3867–3877.

of the structure-dependent (or nondynamical) correlation effects. In these calculations a “minimal” active space was chosen, built from those orbitals which are most involved in the bond cleavage process. These are, for the reagents, those belonging to the  $\pi$  subsystem adjacent to the  $\sigma$  bond to be cleaved, and the  $\sigma$ ,  $\sigma^*$  couple pertaining to the same bond, populated with a number of electrons (depending on the charge) in every possible way, providing a complete CI. The active spaces so defined by  $n$  electrons in  $m$  orbitals are labeled as  $(n,m)$ , i.e., as (3,4) and (5,4) for the  $\alpha\text{-XH}_3^{+}$  and  $\alpha\text{-XH}_3^{-}$  systems, respectively, and (4,4) for the relevant neutral molecules. Similarly, the active spaces are (5,6) and (7,6) for the  $\text{p-XH}_3^{+}$  and  $\text{p-XH}_3^{-}$  systems, respectively, and (6,6) for the related neutral. As the two silicon radical anions exhibit approximately trigonal-bipyramidal geometries around the silicon atom (with one position occupied by the extra electron), we tested in the  $\alpha\text{-SiH}_3^{-}$  system the extension of the active space used in the optimizations by including that  $\sigma$ ,  $\sigma^*$  couple pertaining to the C–H bond more heavily mixed with the  $\sigma$ ,  $\sigma^*$  couple of the cleaving C–Si bond. This is the axial C–H bond, for the extra electron occupying one equatorial position. The resulting extended active space is labeled (7,6). The geometrical parameters did not vary significantly, and consequently the test was limited to the smaller system.

To obtain approximate reaction energy profiles (Figures 1, 3, 5, and 6) several extra points were defined corresponding to fixed interfragment distances C–X by unconstrained optimizations in the subspace of the remaining parameters. Within the CAS-MCSCF scheme, the electron distribution is discussed in terms of Mulliken group charges. As this part of the study demonstrated a basically monodeterminantal nature of the wave function along the dissociation profiles (see the next section), dynamic correlation effects on the reaction energetics were taken care of through a series of single-point coupled cluster calculations,<sup>33</sup> carried out at the *frozen core* CCSD(T) theory level. The energy differences relevant to the fragmentation reactions were recomputed, for comparative purposes, and only for the four  $\alpha\text{-XH}_3^{+}$  and  $\alpha\text{-XH}_3^{-}$  systems, by multireference second-order perturbative single-point energy calculations.<sup>34</sup> These *frozen-core* CAS( $n,m$ )-PT2/6-311G(2d,p) (radical cations) and 6-311+G(2d,p)<sup>32c,d</sup> (radical anions) calculations

are in principle, as far as the reference wave function is concerned, more consistent with the multiconfigurational geometry optimizations. The results are reported in the next section together with the CCSD(T) results that use the same basis sets, and are close to them (see below). In the case of  $\alpha\text{-SiH}_3^{-}$ , the whole energy profile was redefined, to compare its qualitative features with those obtained at the coupled cluster level. All these results further justify the choice of the CCSD(T) level of theory to define the approximate energy profiles for the dissociation of all the radical ions. In the CCSD(T) calculations, the CAS-MCSCF geometries were utilized, in conjunction with the 6-311G(d) basis set, for the radical cations, or the 6-311+G(d) basis set, for the radical anions.<sup>32c,d</sup> The more important energy differences were further assessed by single-point CCSD(T)/6-311G(2d,p) and 6-311+G(2d,p) calculations (the latter in the case of the radical anions).<sup>32c,d</sup> The GAUSSIAN98 suite of programs<sup>35</sup> was used in the CAS-MCSCF geometry optimizations, whereas the CAS-MCSCF + CAS-PT2 single-point energy calculations were done with the MOLCAS 4 program.<sup>36</sup>

## Results and Discussion

The following questions have been addressed. (A) Given that the  $\sigma$  bond cleavage process can produce in principle two fragments with a different partitioning of electric charge and unpaired electron, which is the preferred dissociation mode? (B) Does the expected intervention of an avoided crossing<sup>37</sup> play an important role in contributing to the dissociation barrier? Will it generate an energy barrier for the reverse process (kinetic overhead<sup>10b,c</sup>), or will this feature be masked by relatively large energy differences between each reactant and the resulting fragments? (C) To what extent will fragmentation be activated by electron loss or gain? (D) What is the nature of the dissociation process in the radical cations and radical anions, and how does it compare to homolysis and heterolysis? Finally, making reference to the above points, it will be seen if the methyl and silyl systems exhibit any different features.

In the reagents, the active space consists of the two (or four)-term  $\pi$  system of the double carbon–carbon bonds and the  $\sigma$  system of the bond to be cleaved (as shown in Scheme 3a for the smaller system). These orbitals correlate, in the separated products, to the 3-orbital  $\pi$  (or 5-orbital) system of the resulting allyl (pentadienyl) moiety (Scheme 3b) and to either a p orbital

(30) Schlegel, H. B. In *Computational Theoretical Organic Chemistry*; Csizsmedia, I. G., Daudel, R., Eds.; Reidel Publishing Co.: Hingham, MA, 1981; pp 129–159. Schlegel, H. B. *J. Chem. Phys.* **1982**, *77*, 3676–3681. Schlegel, H. B.; Binkley, J. S.; Pople, J. A. *J. Chem. Phys.* **1984**, *80*, 1976–1981. Schlegel, H. B. *J. Comput. Chem.* **1982**, *3*, 214–218.

(31) Hegarty, D.; Robb, M. A. *Mol. Phys.* **1979**, *38*, 1795–1812.

(32) (a) Hehre, W. J.; Ditchfield, R.; Pople, J. A. *J. Chem. Phys.* **1972**, *56*, 2257–2261. (b) Hariharan, P. C.; Pople, J. A. *Theor. Chim. Acta* **1973**, *28*, 213–222. (c) Clark, T.; Chandrasekhar, J.; Spitznagel, G. W.; Schleyer, P. v. R. *J. Comput. Chem.* **1983**, *4*, 294–301. (d) Krishnan, R.; Binkley, J. S.; Seeger, R.; Pople, J. A. *J. Chem. Phys.* **1980**, *72*, 4256–4266.

(33) Coester, F.; Kümmel, H. *Nucl. Phys.* **1960**, *17*, 477. Cizek, J. *J. Chem. Phys.* **1966**, *45*, 650–654. Paldus, J.; Cizek, J.; Shavitt, I. *Phys. Rev. A* **1972**, *5*, 50–67. Pople, J. A.; Krishnan, R.; Schlegel, H. B.; Binkley, J. S. *Int. J. Quantum Chem.* **1978**, *14*, 545–560. Bartlett, R. J.; Purvis, G. D. *Int. J. Quantum Chem.* **1978**, *14*, 561–581. Cizek, J.; Paldus, J. *Phys. Scr.* **1980**, *21*, 251–254. Bartlett, R. J. *Annu. Rev. Phys. Chem.* **1981**, *32*, 359–401. Purvis, G. D.; Bartlett, R. J. *J. Chem. Phys.* **1982**, *76*, 1910–1918. Scuseria, G. E.; Janssen, C. L.; Schaefer, H. F., III *J. Chem. Phys.* **1988**, *89*, 7382–7387. Scuseria, G. E.; Schaefer, H. F., III *J. Chem. Phys.* **1989**, *90*, 3700–3703. (b) While CAS-MCSCF calculations are expected to provide qualitatively reliable geometries through the inclusion of a significant share of the structure-dependent (nondynamical) correlation energy, CCSD(T) energy evaluations should be more liable for assessing energy differences by inclusion of the dynamical contribution to the correlation energy. It must be prudently kept in mind, however, that performing single-point energy calculations, although usual, is in fact a rather rough probing of the higher level energy hypersurface. This remark is particularly reasonable in the case of the transition structures.

(34) Roos, B. O.; Andersson, K.; Fülischer, M. P.; Malmqvist, P.-Å.; Serrano-Andres, L.; Pierloot, K.; Mercham, M. *Adv. Chem. Phys.* **1996**, *93*, 219–331. Andersson, K.; Malmqvist, P.-Å.; Roos, B. O. *J. Chem. Phys.* **1992**, *96*, 1218–1226.

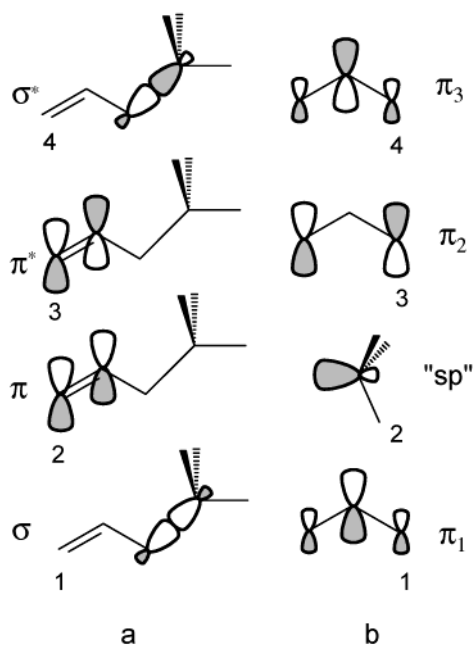
(35) GAUSSIAN 98: Frisch, M. J.; Trucks, G. W.; Schlegel, H. B.; Scuseria, G. E.; Robb, M. A.; Cheeseman, J. R.; Zakrzewski, V. G.; Montgomery, J. A., Jr.; Stratmann, R. E.; Burant, J. C.; Dapprich, S.; Millam, J. M.; Daniels, A. D.; Kudin, K. N.; Strain, M. C.; Farkas, O.; Tomasi, J.; Barone, V.; Cossi, M.; Cammi, R.; Mennucci, B.; Pomelli, C.; Adamo, C.; Clifford, S.; Ochterski, J.; Petersson, G. A.; Ayala, P. Y.; Cui, Q.; Morokuma, K.; Malick, D. K.; Rabuck, A. D.; Raghavachari, K.; Foresman, J. B.; Cioslowski, J.; Ortiz, J. V.; Stefanov, B. B.; Liu, G.; Liashenko, A.; Piskorz, P.; Komaromi, I.; Gomperts, R.; Martin, R. L.; Fox, D. J.; Keith, T.; Al-Laham, M. A.; Peng, C. Y.; Nanayakkara, A.; Gonzalez, C.; Challacombe, M.; Gill, P. M. W.; Johnson, B.; Chen, W.; Wong, M. W.; Andres, J. L.; Gonzalez, C.; Head-Gordon, M.; Replogle, E. S.; Pople, J. A. *GAUSSIAN 98*, Revision A.6; Gaussian, Inc.: Pittsburgh, PA, 1998.

(36) MOLCAS 4: Andersson, K.; Blomberg, M. R. A.; Fülischer, M. P.; Karlström, K.; Lindh, R.; Malmqvist, P.-Å.; Neogrády, P.; Olsen, J.; Roos, B. O.; Sadlej, A. J.; Schütz, M.; Seijo, L.; Serrano-Andres, L.; Siegbahn, P. E. M.; Windmark, P.-O. *MOLCAS*, Version 4: University of Lund: Lund, Sweden, 1997.

(37) Salem, L. *Electrons in Chemical Reactions. First Principles*; J. Wiley & Sons: New York, 1982; pp 141–143 and 148–151. See also, for instance: Pross, A. *Theoretical and Physical Principles of Organic Reactivity*; John Wiley & Sons: New York, 1995; pp 109–121 (and references therein). Shaik, S. S.; Hiberty, P. C. *Adv. Quantum Chem.* **1995**, *26*, 99–163.



## SCHEME 3



of the radical or cationic  $\text{XH}_3$  moiety or to some  $s\text{-}p$  hybrid in the  $\text{XH}_3$  anion (labeled "sp").

The first set of calculations, carried out at the CAS-MCSCF level of theory, has the purpose of providing easily readable wave functions, apt to support a qualitative description and interpretation of the cleavage processes. As the CAS-MCSCF calculations take care only of nondynamical correlation effects, a better assessment of the energy differences is achievable at the coupled cluster level of theory, by using the CAS-MCSCF geometries. Therefore, the CCSD(T) energy difference estimates will be discussed in the following.

**1.  $\text{CH}_2\text{CHCH}_2\text{-XH}_3$  Radical Cations.** The fragmentation of the radical cations of but-1-ene ( $\text{X} = \text{C}$ ) and allylsilane ( $\text{X} = \text{Si}$ ) gives an allyl cation fragment and a methyl or silyl radical. The formation of an allyl radical and a methyl or silyl cation is less favored by significantly different amounts: 40.6 or 2.6  $\text{kcal mol}^{-1}$ , respectively (CCSD(T)/6-311G(2d,p) estimates: see the Supporting Information, file Mesolysis-Excel\_Eplots.xls). These numbers can be compared with the energy differences that can be obtained by using the experimental ionization energies of the methyl, allyl, and silyl radicals.<sup>38–41</sup> The difference is 37.4 for  $\alpha\text{-CH}_3^+$  and ranges from  $-4.2$  to 12.0  $\text{kcal mol}^{-1}$  for  $\alpha\text{-SiH}_3^+$ , respectively.

Bond cleavage in both methyl and silyl systems proceeds without passing through a transition structure

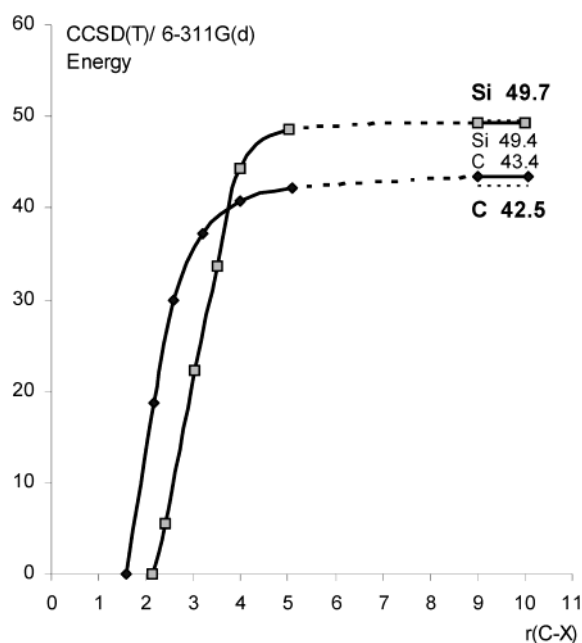


**FIGURE 1.** CCSD(T)/6-311G(d) dissociation energy profile for the  $\text{CH}_2=\text{CHCH}_2\text{-CH}_3^{\bullet+}$  radical cation (black diamonds) and for the  $\text{CH}_2=\text{CHCH}_2\text{-SiH}_3^{\bullet+}$  radical cation (gray squares). Energy values in  $\text{kcal mol}^{-1}$ ,  $\text{C-X}$  distance values in angstroms. Right side: the two smaller numbers are relevant to the terminal part of the energy profiles (continuous segments); the two larger numbers and thin dashed segments represent the CCSD(T)/6-311G(2d,p) dissociation energy assessments.

(Figure 1). In other words, no energy barrier is encountered in the reverse process.

It can be seen that dissociation of the two radical cations into an allyl cation and a methyl or silyl radical takes place by overcoming large energy barriers, coincident with the reaction energies, and is easier in the methyl-substituted system than in the silyl system by only 7  $\text{kcal mol}^{-1}$  at the CCSD(T)/6-311G(2d,p) level (42.5 vs 49.7  $\text{kcal mol}^{-1}$ ). The relevant CAS-PT2 estimates are 42.8 and 53.5, with the same basis set. The first number can be compared both to the MP2/6-31G(d)//UHF/6-31G(d) result of Du et al.,<sup>22</sup> 43.7  $\text{kcal mol}^{-1}$ , and to the value that can be computed from experimental thermochemical data, 40–41  $\text{kcal mol}^{-1}$ .<sup>22,38</sup>

**Activation toward Dissociation.** The coupled cluster data for the radical ions and their fragmentation products show that both reactions are remarkably activated with respect to the similar homolytic process in the neutral systems. Homolysis of but-1-ene and allylsilane requires very large energies (as computed with the same basis set used for the radical cations): 81  $\text{kcal mol}^{-1}$  (compare 74  $\text{kcal mol}^{-1}$ , from thermochemical data),<sup>38</sup> and 73  $\text{kcal mol}^{-1}$ , respectively (for Si no experimental datum has been found). See Scheme 4, right, numbers in italic and dashed arrow.

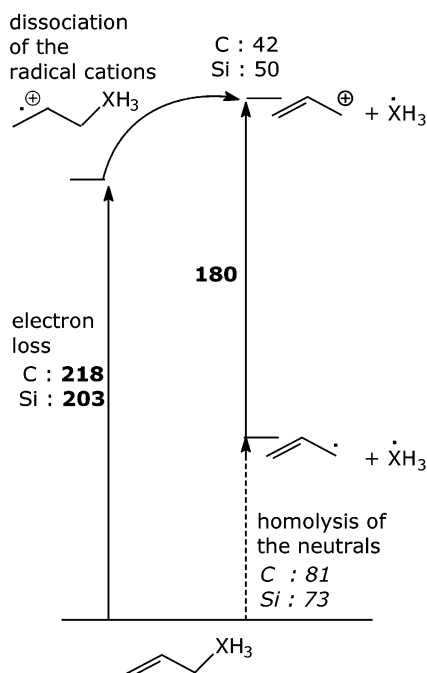
(38) Lias, S. G.; Bartmess, J. E.; Liebman, J. F.; Holmes, J. L.; Levin, R. D.; Mallard, W. G. *J. Phys. Chem. Ref. Data Suppl.* **1988**, *17*. Compare also the IE and EA data available on the NIST site (<http://webbook.nist.gov/>).

(39) Methyl, IE = 9.84 eV, from: Berkowitz, J.; Ellison, G. B.; Gutman, D. *J. Phys. Chem.* **1994**, *98*, 2744. Nagano, Y.; Murthy, S.; Beauchamp, J. L. *J. Am. Chem. Soc.* **1993**, *115*, 10805. EA = 0.08 eV, from: Ellison, G. B.; Engelking, P. C.; Lineberger, W. C. *J. Am. Chem. Soc.*, **1978**, *100*, 2556.

(40) Allyl, IE = 8.18 eV, from: Kagramanov, N. D.; Ujjaszsy, K.; Tamas, J.; Mal'tsev, A. K.; Nefedov, O. M. *Bull. Acad. Sci. USSR, Div. Chem. Sci.* **1983**, *7*, 1531 (in original 1683). EA = 0.481 eV, from: Wenthold, P. G.; Polak, M. L.; Lineberger, W. C. *J. Phys. Chem.*, **1996**, *100*, 6920.

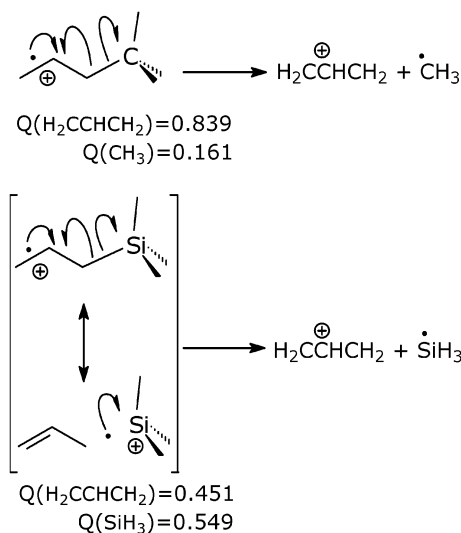
(41) Silyl, IE = 8.01–8.17 eV, from: Nagano, Y.; Murthy, S.; Beauchamp, J. L. *J. Am. Chem. Soc.* **1993**, *115*, 10805. Johnson, R. D., III; Tsai, B. P.; Hudgens, J. W. *J. Chem. Phys.* **1989**, *91*, 3340. Boo, B. H.; Armentrout, P. B. *J. Am. Chem. Soc.* **1987**, *109*, 3549. Berkowitz, J.; Greene, J. P.; Cho, H.; Ruscic, B. *J. Chem. Phys.* **1987**, *86*, 1235. EA = 1.406 eV, from: Wetzel, D. M.; Salomon, K. E.; Berger, S.; Brauman, J. I. *J. Am. Chem. Soc.*, **1989**, *111*, 3835. Nimlos, M. R.; Ellison, G. B. *J. Am. Chem. Soc.*, **1986**, *108*, 6522.

## SCHEME 4



Fragmentation of the corresponding radical cations demands, if we consider the reaction energies, 42 and 50 kcal mol<sup>-1</sup> (Scheme 4, upper curved arrow). As in the case of the two radical cations, both homolytic dissociation profiles are entirely determined by the reaction energies and do not show a barrier for the reverse process. Considering the energetics of these dissociations, it can be seen, on one hand, that the radical cations are higher in energy than the neutrals by a considerable amount, estimated, at the same computational level, as large as 218 (methyl) and 203 kcal mol<sup>-1</sup> (silyl) (Scheme 4, leftmost arrow). A comparison of these numbers with experimental IE data is possible: 220 (methyl) and 196 kcal mol<sup>-1</sup> (silyl).<sup>38,44a</sup> On the other hand, the dissociation limits (radical cations vs neutrals) are separated by 180 kcal mol<sup>-1</sup>, while 189 kcal mol<sup>-1</sup> is the value obtainable from IE data.<sup>38,40</sup> This corresponds to the energy difference between allyl<sup>+</sup> and allyl<sup>•</sup> (rightmost arrow and bold number). The two differences between the dissociation energies, -38 (methyl) or -23 kcal mol<sup>-1</sup> (silyl), put the

## SCHEME 5



fragmentation of the radical cations on a better ground with respect to the neutrals (“activation” toward fragmentation). The estimate obtainable for the methyl case from thermochemical data is -34 kcal mol<sup>-1</sup>.<sup>38</sup> Thus, an important contribution to cleavage activation comes from the fact that the reactant energy level is raised by removal of one electron, but the product side is destabilized to a lesser extent.

**Nature of the Dissociation.** The dissociation that takes place in the two radical cations can be sketched at first as homolytic (Scheme 5, top and middle drawings), though it has to be kept in mind that in both cases one of the electrons involved couples its spin with that of the originally unpaired electron.

At the onset, the electron distribution in the two reactant systems is different. In the carbon case, the positive charge is more localized on what will become the allyl cationic fragment, while in the silicon case the charge is divided much more evenly between the two potential fragments. So, a second limit form can be drawn (only for Si), as shown in Scheme 5, bottom. As concerns the cleavage process, the single structure drawn for carbon and the first limit form drawn for silicon state that two electrons have to become spin-coupled (left and middle arrows) as the bond cleaves (middle and right arrows). The second limit form of the silicon radical cation describes this coupling as already accomplished in the reactant ( $\pi$  bond). The spin recoupling appears to be central to both carbon and silicon processes.

The charge distribution in the reactant radical cations has a counterpart in the variations of the main geometrical parameters with respect to the neutral precursors (Table 1). For instance, the silicon system exhibits rather large variations that hint to some hyperconjugative effect (C-Si distance: +10%; CCSi angle: -10%). The carbon radical cation has more modest deviations in the same direction (C<sup>3</sup>-C<sup>4</sup>: +1%, CCC<sup>4</sup>: -6%). Similarly, as a consequence of hyperconjugation, the C<sup>2</sup>-C<sup>3</sup> bond adjacent to the XH<sub>3</sub> group gets shorter by -7% (X = Si) or by -3% (X = C), while the C<sup>1</sup>-C<sup>2</sup> bond length (depleted of some electron population) shows a +5% increase in both cases.

(42) Pentadienyl, IE = 7.25 eV, from: Lossing, F. P.; Traeger, J. C. *J. Am. Chem. Soc.* **1975**, *97*, 9. EA = 0.91 eV, from: Zimmerman, A. H.; Gygax, R.; Brauman, J. I. *J. Am. Chem. Soc.* **1978**, *100*, 5595.

(43) When the computed energy differences between the anions and the corresponding radicals are compared with the experimental electron affinity values, they are lower in all cases. Methyl:  $E(\text{CH}_3^\ominus) - E(\text{CH}_3^\bullet) = -7.0$  vs EA =  $1.8 \pm 0.7$  kcal mol<sup>-1</sup>. Silyl:  $E(\text{SiH}_3^\ominus) - E(\text{SiH}_3^\bullet) = 25$  vs EA =  $32.45 \pm 0.32$  kcal mol<sup>-1</sup>. Allyl:  $E(\text{a}^\ominus) - E(\text{a}^\bullet) = 2$  vs EA =  $11.1 \pm 0.18$  kcal mol<sup>-1</sup>. Pentadienyl:  $E(\text{p}^\ominus) - E(\text{p}^\bullet) = 14$  vs EA =  $21.0 \pm 0.7$  kcal mol<sup>-1</sup>. The discrepancy is largely due to basis set deficiencies. In fact, we carried out some tests on these molecules at the CCSD(T) level with basis sets of increasing size, up to 6-311++G(3df,2p), and found significant improvements in approaching the experimental data. Unfortunately, at the CCSD(T) level, the 6-311+G(2d,p) is the largest affordable basis set for the heaviest systems dealt with in this paper. On the other hand, when estimating either the energy differences between different dissociation limits or the activation effects, some cancellations produce a better agreement with the same values assessed by using the experimental data (compare the Supporting Information, file Mesolysis-Excel\_Eplots.xls).

(44) (a) Van der Meij, C. E.; Van Eck, J.; Niehaus, A. *Chem. Phys.* **1989**, *130*, 325. (b) Wolkoff, P.; Holmes, J. L.; Lossing, F. P. *Can. J. Chem.* **1980**, *58*, 251.

**TABLE 1.** Selected Geometrical Parameters for the  $\alpha$ -XH<sub>3</sub> Reactants

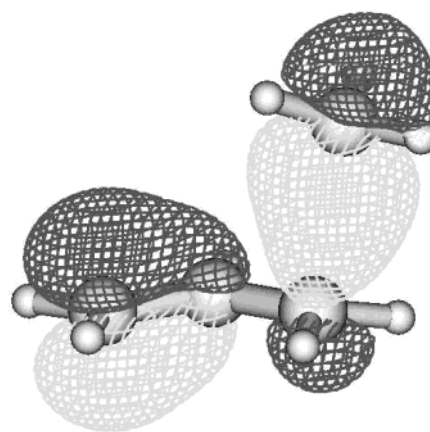
	1-2	2-3	3-4	$\alpha$
neutral	1.339	1.506	1.559	112.4
cation	1.409	1.468	1.586	108.4
anion	1.441	1.512	1.574	115.7

	1-2	2-3	3-4	$\alpha$
neutral	1.340	1.507	1.926	112.7
cation	1.411	1.399	2.116	101.1
anion	1.347	1.485	2.085	112.7

The CI wave function  $\Psi$  provides a complementary ground of analysis, based on a comparison with the features of pure homolytic and heterolytic fragmentations. In the CAS-MSCF calculations a complete CI is carried out within the orbitals belonging to the active space, and the analysis of  $\Psi$  can be done in terms of populations of these active orbitals ( $\gamma_i$ ) or, equivalently, in terms of the highest coefficients of the lowest energy CI eigenvector. In fact, a single configuration is found to dominate  $\Psi$  all along the dissociation pathway, in both  $X = C$  and  $X = Si$  cases. This almost monodeterminantal nature of  $\Psi$  is reflected in fractional populations  $\gamma_i$  rather close to 0, 1, and 2 for the four active orbitals of the (3,4) active space (these features, incidentally, allow us to deem reliable the single-reference coupled cluster assessment of the energy differences). The molecular orbitals 1 and 2 ( $\sigma_{CX}$  and  $\pi_{CC}$  in the  $\alpha$ -CH<sub>3</sub><sup>+</sup> and  $\alpha$ -SiH<sub>3</sub><sup>-</sup> reactants, as shown in Scheme 3) become in-phase and out-of-phase combinations of the same  $\pi_{CC}$  and  $\sigma_{CX}$  orbitals as the C–X bond gets stretched. The electron distribution gets modified from the initial  $\pi_{CC}^1\sigma_{CX}^2$  situation, and the unpaired electron becomes increasingly associated to the initial  $\sigma_{CX}$  orbital (as shown in Figure 2 for the but-1-ene radical cation).

Thus the cleaving  $\sigma$  bond has increasing characteristics of a singly occupied bond, a feature that promotes the cleavage itself. As concerns the populations of the active orbitals, in the  $\alpha$ -CH<sub>3</sub><sup>+</sup> reactant they are  $\gamma_1 = 1.978$ ,  $\gamma_2 = 1.000$ ,  $\gamma_3 = 0.004$ , and  $\gamma_4 = 0.018$ , and correspond to a coefficient of 0.994 for the most important configuration in the CI eigenvector (the numbers 1–4 refer to Scheme 3). In the two-fragment system (10 Å apart) they become  $\gamma_1 = 1.906$ ,  $\gamma_2 = 1.000$ ,  $\gamma_3 = 0.076$ , and  $\gamma_4 = 0.018$  (see Scheme 3, right side), and correspond to a coefficient of 0.976. In  $\alpha$ -SiH<sub>3</sub><sup>-</sup>,  $\gamma_1 = 1.954$ ,  $\gamma_2 = 1.001$ ,  $\gamma_3 = 0.031$ , and  $\gamma_4 = 0.014$  correspond to a coefficient of 0.985 for the most important configuration in the CI eigenvector. In the two-fragment silicon system the  $\gamma_i$  and the CI coefficient have just the same values as for carbon. This picture points out that the dissociation process is basically different in nature from homolysis in both  $X = C$  and  $X = Si$  cases: in fact, a homolytic process sees the dominance of two configurations, as the bond is stretched. The spin recoupling of one of the two C–X bond electrons

**FIGURE 2.** The singly occupied active MO of the radical cation of but-1-ene, at a C–X distance of 2.3 Å.

with the unpaired electron is at the origin of the mono-configurational nature of dissociation in the radical cations. This point is further addressed at the end of section 2.

**2. CH<sub>2</sub>CHCH<sub>2</sub>–XH<sub>3</sub> Radical Anions.** Though the two radical anions are present as minima on the energy hypersurface, two calculations on the neutral systems, carried out at the same computational level at the optimized geometries of the radical anions, show that in the gas phase only the silicon radical anion is kinetically stable with respect to electron loss (see the Supporting Information for details). The radical ions could of course benefit from some extra stabilization in the condensed phase, due to the interactions with the counterion and the solvent itself. Notwithstanding this limitation of our gas-phase model hydrocarbon system, the study of the dissociation process has been carried out parallel to that of the silicon system, to address the abovementioned points.

The fragmentation reaction, though still endoergic, is less unfavorable in the radical anions than in the radical cations. The reaction energy is 29.0 kcal mol<sup>-1</sup> in  $\alpha$ -CH<sub>3</sub><sup>-</sup>, and 12.9 kcal mol<sup>-1</sup> in  $\alpha$ -SiH<sub>3</sub><sup>-</sup>. In  $\alpha$ -CH<sub>3</sub><sup>-</sup> the tetrahedral methyl group owns a minor share of the negative charge ( $Q_{\text{Mulliken}} = -0.111$  e). The fragmentation of the radical anion of but-1-ene produces an allyl anion fragment and a methyl radical. The opposite dissociation mode produces an allyl radical fragment and a methyl anion that are 9.2 kcal mol<sup>-1</sup> higher in energy. This result can be compared with the energy difference obtained from the experimental electron affinities of the methyl and allyl radicals, 9.3 kcal mol<sup>-1</sup>.<sup>38–40</sup> By contrast, the fragmentation of  $\alpha$ -SiH<sub>3</sub><sup>-</sup> (in which the extra electron is more localized on the almost trigonal bipyramidal SiH<sub>3</sub> group,  $Q_{\text{Mulliken}} = -0.520$  e) produces an allyl radical fragment and a silyl anion. The allyl anion plus silyl radical couple is 22.9 kcal mol<sup>-1</sup> higher in energy. By using the experimental electron affinities of the allyl and silyl radicals,<sup>38,40,41</sup> a value of 21.4–22.1 kcal mol<sup>-1</sup> is obtained for comparison. The fairly good agreement is due in fact to some cancellation of errors.<sup>43</sup>

Bond cleavage proceeds in both systems by passing through transition structures (Figure 3), but the energy maximum is lower than the dissociation limit. Dissociation of the two radical anions takes place by overcoming



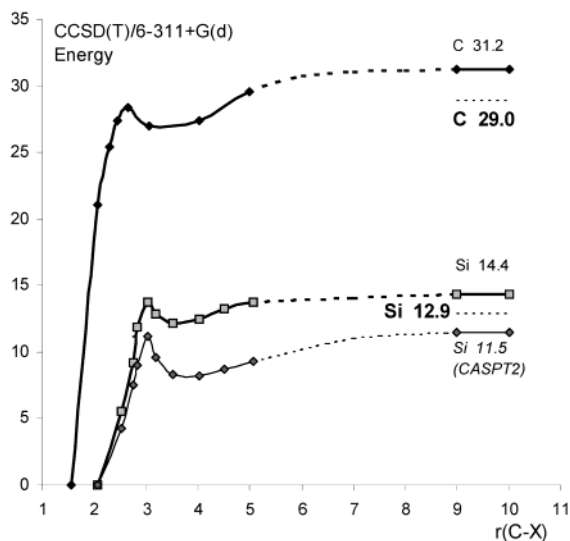
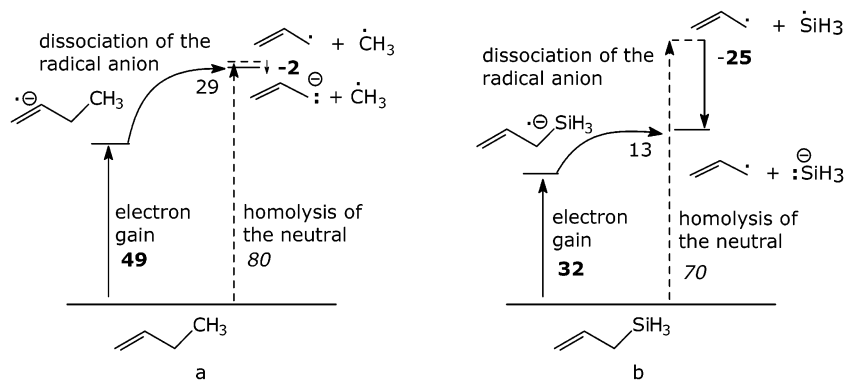


**FIGURE 3.** CCSD(T)/6-311+G(d) dissociation energy profile for the  $\text{CH}_2=\text{CHCH}_2\text{-CH}_3^{\bullet-}$  radical anion (black diamonds) and for the  $\text{CH}_2=\text{CHCH}_2\text{-SiH}_3^{\bullet-}$  radical anion (gray squares). Energy values in  $\text{kcal mol}^{-1}$ , C-X distance values in angstroms. Right side: the two smaller numbers are relevant to the terminal part of the energy profiles (continuous segments); the two larger numbers and thin dashed segments represent the CCSD(T)/6-311+G(2d,p) dissociation energy assessments. The lowest energy profile is the CAS(7,6)-PT2/6-311+G(d).

energy barriers which are smaller than those for the radical cations. The reaction energy is lower in the silyl-substituted system ( $12.9 \text{ kcal mol}^{-1}$ ) than in the methyl ( $29.0 \text{ kcal mol}^{-1}$ ). The CAS-PT2 estimates are  $12.1$  and  $31.6 \text{ kcal mol}^{-1}$ , respectively, with the same basis set (see the Supporting Information for further details). The qualitative features of the CAS-PT2 energy profile are close to those of the CCSD(T) profile.

**Activation toward Dissociation.** Also the radical anion dissociations are activated with respect to the homolytic process in the neutral systems. The homolysis of but-1-ene and allylsilane requires, with the 6-311+G-(2d,p) basis set,  $80$  ( $74 \text{ kcal mol}^{-1}$  is the thermochemical estimate) or  $70 \text{ kcal mol}^{-1}$ , respectively (Scheme 6, a and b, respectively, numbers in italic, dashed arrows and energy levels). By contrast, fragmentation of the corresponding radical anions demands overcoming the barriers of only  $29$  and  $13 \text{ kcal mol}^{-1}$ . It can be seen that the radical anions are higher in energy than the neutrals by  $49$  (methyl) and  $32 \text{ kcal mol}^{-1}$  (silyl), at the same

#### SCHEME 6



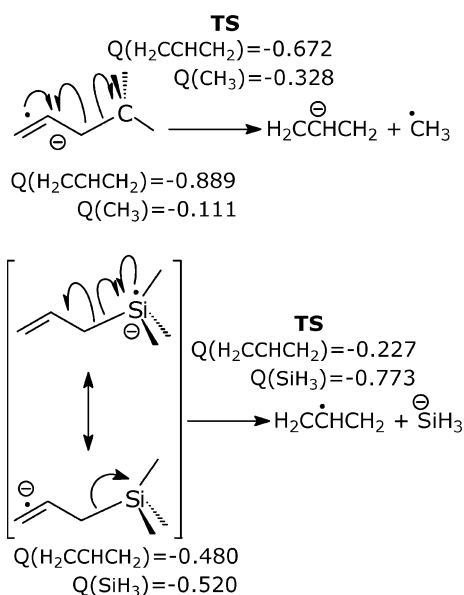
computational level (Scheme 6, a and b, respectively, leftmost arrows). The two methyl dissociation limits (radical anion vs neutral) are rather close: they are separated by  $2 \text{ kcal mol}^{-1}$  (bold italic number), i.e., by the computed energy difference between the more stable allyl anion and the allyl radical. For silyl dissociation, the limit defined by the allyl radical and silide is lower than the homolytic by  $25 \text{ kcal mol}^{-1}$  (bold italic number and downward arrow), i.e., by the energy difference between silide and silyl. The two computed energy differences are rather small, if compared to the experimental allyl and silyl EA values,  $11$  and  $32 \text{ kcal mol}^{-1}$ , respectively.<sup>40,41,43,44</sup> The combination of these data brings about a sizable “activation” effect in the radical anions:  $-51$  (C) or  $-57 \text{ kcal mol}^{-1}$  (Si) with respect to the homolysis of the corresponding neutrals. This is larger than that estimated for the corresponding radical cations ( $-40$  and  $-25 \text{ kcal mol}^{-1}$ , respectively). The origin of cleavage activation is mainly due to the reactant destabilization, especially in the carbon case. Though the present computations, when compared to the experiments, underestimate the allyl and silyl EA’s (see the Supporting Information), a similar underestimation could be present for the radical anion reactants (for which no experimental datum is available). The upward shift of both energy levels would limit the error in the estimate of the activation effect. No experimental EA data have been found for the parent neutrals.

**Nature of the Dissociation.** It can be seen (Scheme 7, top drawing) that in the  $\text{a-CH}_3^{\bullet-}$  reactant the charge is more evidently localized on the to-be ionic fragment, while in the  $\text{a-SiH}_3^{\bullet-}$  reactant the charge is divided almost evenly between the potential fragments. This suggests that only in the Si reactant can a second limit form be written down (Scheme 7, middle and bottom drawings).

If the dissociation mode of  $\text{a-SiH}_3^{\bullet-}$  into  $\text{a}^{\bullet}$  and  $\text{SiH}_3^-$  is taken into account, the upper Si resonance structure indicates homolytic cleavage, as for  $\text{a-CH}_3^{\bullet-}$ , while the bottom structure, similar to that of carbon as regards the electron distribution, suggests heterolytic cleavage. Thus, if defining the fragmentation of the carbon radical anion as homolysis would seem on this basis rather acceptable, this is not the case for the silicon radical anion, for which the situation is less clear-cut. Scheme 5 can be compared: in both a spin recoupling pattern can be seen.

Here again, the charge distribution in the reactant radical anions is reflected by the variations of the more

## SCHEME 7



important geometrical parameters with respect to the neutral parent molecules (Table 1). The silicon-centered group undergoes in this case a significant change. The HSiC angles (166°, 94°, 93°) show that its geometry approaches a trigonal-bipyramidal arrangement, with the extra electron mostly localized in an equatorial position: as a consequence the axial C–Si bond stretches by +8%. By contrast, as the carbon system bears the extra electron on the former double bond, it is this bond that is elongated (by the same percent). The consequences of the addition of one electron seem to be more localized on the C<sup>1</sup>–C<sup>2</sup> bond with respect to what is observed (Table 1) in the related radical cation.

The features of the CI wave function  $\Psi$  offer a complementary ground of scrutiny, based on the corresponding features of a sheer homolytic or heterolytic cleavage. The analysis is done again in terms of coefficients of the lowest eigenvector and populations of the active orbitals ( $\gamma_i$ ). A single configuration stands out at all interfragment distances, and the fractional populations of the active orbitals  $\gamma_i$  are rather close to 0, 1, and 2. For instance, in the methyl dissociation TS of but-1-ene<sup>•-</sup>,  $\gamma_1 = 1.981$ ,  $\gamma_2 = 1.941$ ,  $\gamma_3 = 1.007$ , and  $\gamma_4 = 0.070$ . These data correspond to a 0.973 coefficient for the dominant configuration in  $\Psi$ . The silyl system behaves similarly (for instance, the largest CI coefficient in the TS is 0.961), though its fragmentation mode is opposite. This picture is clearly different from what is characteristic of homolysis (two-electron configurations acquiring comparable weight as the bond is stretched). On this basis, the dissociation mode for a-SiH<sub>3</sub><sup>•-</sup> could seem closer to heterolysis, in which no electron pair is disrupted and one configuration dominates at all distances. However, as seen for the radical cations, the spin pairing of the originally unpaired electron with one of the electrons of the cleaving bond is a very important feature, which can be responsible on its own for the monoconfigurational nature of  $\Psi$ . This trait of  $\Psi$  is present not only for the silicon system, but also for carbon. The description appears endowed with some ambiguity and seems to

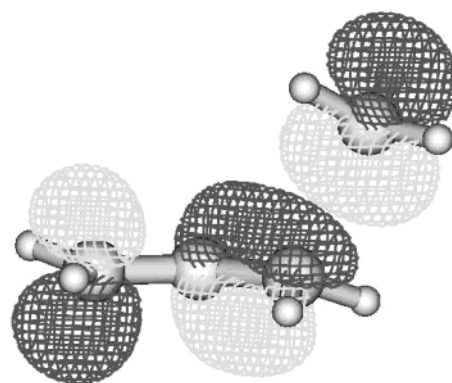


**FIGURE 4.** The singly occupied active MO of the radical anion of but-1-ene, at a C–X distance of 2.3 Å, that corresponds to the CAS-MCSCF dissociation TS.

justify on an even larger acceptance the label *mesolysis* originally proposed by Maslak for this kind of process.<sup>10a</sup>

In the TS, the initially localized active molecular orbitals become in-phase and out-of-phase combinations of the  $\pi$  and  $\sigma$  orbitals. This situation evolves, with the increasing C–XH<sub>3</sub> distance, toward one in which the single electron occupies an orbital largely characterized by the contribution of the  $\sigma_{\text{CX}}^*$  component (as shown in Figure 4 for the radical anion of but-1-ene). This feature clearly favors the cleavage of the  $\sigma$  bond.

The spin recoupling of one of the two C–X bond electrons with the unpaired electron makes the difference for both the radical cation and radical anion cases with respect to the analogous neutral molecules. Scheme 8 helps in illustrating where the difference lies. This simple picture points out that the dissociation process, which can be formally drawn and thought of as homolytic (or in some respect heterolytic, depending on the case), is basically different in nature from these two limits. As the C–X bond stretches, the  $\sigma_{\text{CX}}$  and  $\sigma_{\text{CX}}^*$  orbitals come closer in energy, while becoming more localized on the two separating fragments (“p(C)” and “p(X)”). In a homolytic process this near-degeneracy implies the comparable weight of two electron configurations (Scheme 8, left). In the case of mesolysis, a singly occupied orbital is present on the  $\pi$  fragment (a  $\pi$  orbital for a radical cation, or a  $\pi^*$  orbital for a radical anion). This is close in energy to the “p(C)” on the carbon involved in the bond cleavage, and overlaps well with it. The resulting spin coupling allows a single electron configuration to dominate the wave function (Scheme 8, right).

**3. CH<sub>2</sub>=CH–CH=CH<sub>2</sub>–XH<sub>3</sub> Radical Cations.** For the hexa-1,3-dienyl system, p-CH<sub>3</sub><sup>•+</sup>, fragmentation gives a pentadienyl cation fragment and a methyl radical. The fragmentation to pentadienyl radical and methyl cation is less favored by 58.4 kcal mol<sup>-1</sup>. For the radical cation of penta-2,4-dienylsilane, p-SiH<sub>3</sub><sup>•+</sup>, a similar fragmentation takes place, and the less favored dissociation limit (pentadienyl radical + silyl cation) is 20.4 kcal mol<sup>-1</sup> higher. These numbers can be compared with the energy differences provided by the experimental ionization energies of the methyl, silyl, and pentadienyl radicals,<sup>38,39,41,42</sup> which are 58.9 and 17.6–21.3 kcal mol<sup>-1</sup>, respectively. The two reactants exhibit a different electron distribution. In p-CH<sub>3</sub><sup>•+</sup> the charge is more localized on what will become the pentadienyl cationic fragment ( $Q_{\text{Mulliken}} =$



## SCHEME 8

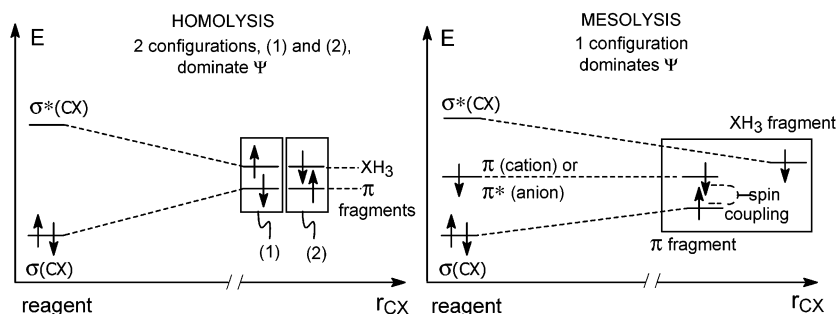


**TABLE 2. Selected Geometrical Parameters for the p-XH<sub>3</sub> Reactants**

	1-2	2-3	3-4	4-5	5-6	α
neutral	1.344	1.465	1.345	1.505	1.558	112.4
cation	1.385	1.397	1.392	1.484	1.572	111.1
anion	1.380	1.402	1.405	1.504	1.571	115.1

	1-2	2-3	3-4	4-5	5-6	α
neutral	1.344	1.464	1.356	1.505	1.926	112.8
cation	1.382	1.399	1.400	1.439	2.010	109.1
anion	1.349	1.457	1.356	1.472	2.114	111.4

0.114 e for the methyl group). By contrast, in p-SiH<sub>3</sub><sup>+</sup> the charge is divided much more evenly between the two potential fragments ( $Q_{\text{Mulliken}} = 0.429$  e). These traits are similar to those shown by a-CH<sub>3</sub><sup>+</sup> and a-SiH<sub>3</sub><sup>+</sup>, though the more extended π-system is now able to tolerate a somewhat larger share of the positive charge.

Table 2 show that the C–Si bond stretches by 4% in p-SiH<sub>3</sub><sup>+</sup> (while the elongation was +10% in a-SiH<sub>3</sub><sup>+</sup>), and the CCSi angle is reduced by 3% (to be compared with –10% in a-SiH<sub>3</sub><sup>+</sup>). Similarly, the single C–C bond adjacent to the SiH<sub>3</sub> group gets shorter by 4% (–7% in a-SiH<sub>3</sub><sup>+</sup>). Though both the geometry and the charge distribution are consistent with some hyperconjugation effect, this seems to be less pronounced than in the smaller system. As regards the p-CH<sub>3</sub><sup>+</sup> system, such an effect is absent.

To dissociate into a pentadienyl cation and a methyl or silyl radical, the two radical cations have to overcome large energy barriers that almost correspond to the reaction energies. In fact, for p-CH<sub>3</sub><sup>+</sup>, the energy profile for C–X bond cleavage presents a quite flat surface and no barrier to reassociation. The p-SiH<sub>3</sub><sup>+</sup> system presents a modest reassociation barrier, ca. 1 kcal mol<sup>–1</sup> high (Figure 5). At the CCSD(T) level the reaction energies are very close in the methyl and silyl systems (46.2 and 46.3 kcal mol<sup>–1</sup>). The datum for the methyl system can be compared with the estimate obtainable from thermochemical data,<sup>38</sup> 45 kcal mol<sup>–1</sup>.

**Activation toward Dissociation.** Both reactions are activated with respect to the similar homolytic process in the neutral systems. The situation is sketched in Scheme 9 for both radical cations. Homolysis of hexa-1,3-diene and penta-2,4-dienylsilane requires very large energies, 76 (compare 74 kcal mol<sup>–1</sup>, from thermochemical data)<sup>38</sup> and 68 kcal mol<sup>–1</sup>, respectively (Scheme 9, bottom, numbers in italic and dashed arrow). Both dissociation profiles are entirely determined by the reaction energies and do not show a barrier for the reverse process. Fragmentation of either radical cation (Scheme 9, upper curved arrow) demands 46 kcal mol<sup>–1</sup>. From the energetics of these dissociations, it can be seen that the radical cations are higher in energy than the neutrals by a large amount, but not as much as their allyl counterparts (Scheme 9, leftmost arrow): 192 (C) (comparable with the estimate obtainable from thermochemical data,<sup>38</sup> 197 kcal mol<sup>–1</sup>) and 184 kcal mol<sup>–1</sup> (Si, for which no experimental IE has been found). The dissocia-

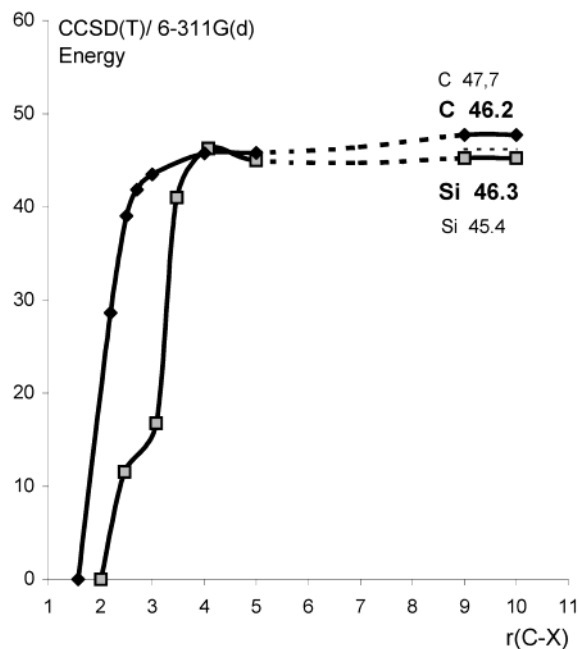
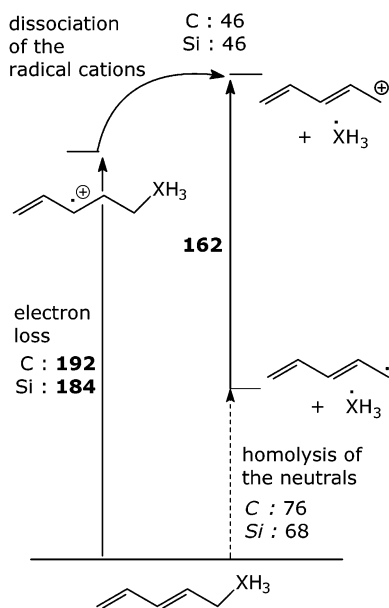


**FIGURE 5.** CCSD(T) dissociation energy profile for the CH<sub>2</sub>=CHCH=CHCH<sub>2</sub>–CH<sub>3</sub><sup>+</sup> radical cation (black diamonds) and for the CH<sub>2</sub>=CHCH=CHCH<sub>2</sub>–SiH<sub>3</sub><sup>+</sup> radical cation (gray squares). Energy values in kcal mol<sup>–1</sup>, C–X distance values in angstroms. Right side: the two smaller numbers are relevant to the terminal part of the energy profiles (continuous segments); the two larger numbers and thin dashed segments represent the CCSD(T)/6-311G(2d,p) dissociation energy assessments.

## SCHEME 9



tion limits are separated in both cases by 162 kcal mol<sup>-1</sup> (i.e. by the energy difference between pentadienyl<sup>+</sup> and pentadienyl<sup>•</sup>), 18 kcal mol<sup>-1</sup> less than what was found for the allyl systems. This datum is comparable again with the thermochemical estimate,<sup>38,44b</sup> 167 kcal mol<sup>-1</sup>. The data bring about an “activation” effect, with respect to homolysis in the neutrals, of -30 (methyl) or -22 (silyl) kcal mol<sup>-1</sup>. In the analogous allyl systems these estimates were -38 (methyl) and -23 kcal mol<sup>-1</sup> (silyl). The estimate of the activation effect computed for the methyl system is quite close to the thermochemical datum,<sup>38</sup> -29 kcal mol<sup>-1</sup>.

**Nature of the Dissociation.** From the examination of the CI wave function  $\Psi$ , a single configuration emerges as dominating at all distances. As an example, in the methyl dissociation TS of p-CH<sub>3</sub><sup>+</sup> (occurring at  $r_{CC} = 2.70$  Å),  $\gamma_1 = 1.936$ ,  $\gamma_2 = 1.890$ ,  $\gamma_3 = 1.001$ ,  $\gamma_4 = 0.099$ ,  $\gamma_5 = 0.053$ , and  $\gamma_6 = 0.021$ , which correspond to a 0.953 coefficient for the dominant configuration in  $\Psi$ . The same comments formulated for the analogous allylic systems hold, and will not be repeated here.

**4. CH<sub>2</sub>=CH-CH=CH<sub>2</sub>-XH<sub>3</sub> Radical Anions.** As was the case for the smaller radical anions (subsection 2), only the silicon one is kinetically stable with respect to electron loss (see the Supporting Information for details). This is admittedly a limitation of our model hydrocarbon system; however, the study of its dissociation (carried out parallel to that of its silicon analogue) is helpful for addressing the points mentioned at the beginning of this section.

In p-CH<sub>3</sub><sup>-</sup> only a minor part of the negative charge is associated to the tetrahedral methyl group ( $Q_{\text{Mulliken}} = -0.085$  e), similarly to a-CH<sub>3</sub><sup>-</sup>, but the more extended  $\pi$ -system is evidently a better acceptor. The fragmentation of the radical anion p-CH<sub>3</sub><sup>-</sup> produces a pentadienyl anion fragment and a methyl radical. The reverse charge and electron apportionment produces a pentadienyl radical fragment and a methyl anion that are 20.8 kcal mol<sup>-1</sup> higher in energy. This result can be compared with the energy difference of 19.2 kcal mol<sup>-1</sup>, obtained from the

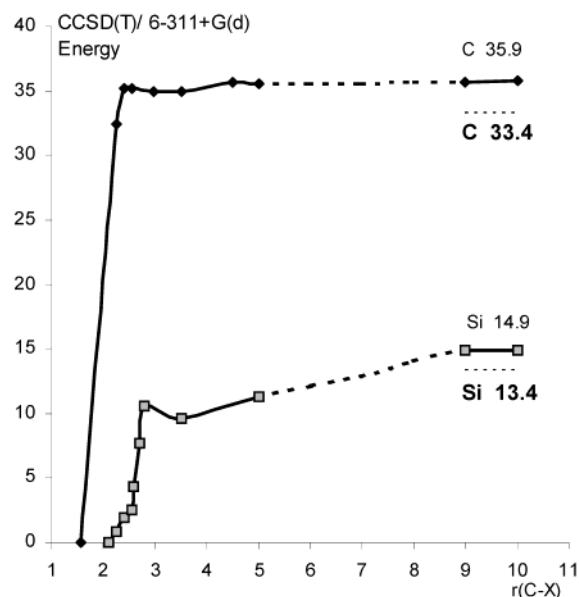


**FIGURE 6.** CCSD(T) dissociation energy profile for the CH<sub>2</sub>=CHCH=CHCH<sub>2</sub>-CH<sub>3</sub><sup>•-</sup> radical anion (black diamonds) and for the CH<sub>2</sub>=CHCH=CHCH<sub>2</sub>-SiH<sub>3</sub><sup>•-</sup> radical anion (gray squares). Energy values in kcal mol<sup>-1</sup>, C-X distance values in angstroms. Right side: the two smaller numbers are relevant to the terminal part of the energy profiles (continuous segments); the two larger numbers and thin dashed segments represent the CCSD(T)/6-311+G(2d,p) dissociation energy assessments.

experimental electron affinities of the methyl and pentadienyl radicals.<sup>38,39,42</sup> By contrast, in p-SiH<sub>3</sub><sup>-</sup> the extra electron is more localized on the almost trigonal bipyramidal XH<sub>3</sub> group ( $Q_{\text{Mulliken}} = -0.492$  e), though not as much as in a-SiH<sub>3</sub><sup>-</sup>.

The silicon-centered group approaches also in this case a trigonal-bipyramidal arrangement (HSiC angles: 165°, 93°, 94°). The extra electron is mostly localized in an equatorial position, and the axial C-Si bond stretches by +10%, while the  $\pi$  system is quite similar to the neutral. By contrast, in p-CH<sub>3</sub><sup>-</sup>, as the  $\pi$  system bears the extra electron, its bonds change by  $\pm 3$ -4% (as in the analogous cation). The C<sup>5</sup>-C<sup>6</sup> bond is stretched by a negligible amount (Table 2).

Its fragmentation produces a pentadienyl radical fragment and a silyl anion, and the pentadienyl anion plus silyl radical couple is 11.1 kcal mol<sup>-1</sup> higher in energy. The experimental electron affinities of the silyl and pentadienyl radicals give a value of 11.5 kcal mol<sup>-1</sup>.<sup>38,41,42</sup> In both cases, the satisfactory agreement is due again to some cancellation of errors.<sup>43</sup> The fragmentation in the radical anions is a less unfavorable process than that in the radical cations, in particular for p-SiH<sub>3</sub><sup>-</sup>. It is endoergic for both systems, by 33.4 kcal mol<sup>-1</sup> in p-CH<sub>3</sub><sup>-</sup> and 13.4 kcal mol<sup>-1</sup> in p-SiH<sub>3</sub><sup>-</sup>. Bond cleavage proceeds in both systems by passing through energy maxima, but these are lower than the dissociation limit, for both C and Si (Figure 6).

**Activation toward Dissociation.** Both C and Si reactions are activated with respect to the similar homolytic process in the neutral systems. Scheme 10 illustrates the situation in both cases. As mentioned in the preceding subsection, homolysis of hexa-1,3-diene and







(D) The qualitative features of the dissociation processes (electron distribution, wave function properties) have been examined within a multiconfiguration approach, to better understand their nature. In the carbon radical ion reactants the charge is more clearly localized on that part of the molecule that will become the ionic fragment. The fragmentation could be formally sketched as homolytic. In the silicon radical ions, by contrast, the charge is partitioned almost equally between the two potential fragments, and the situation is less clear-cut. A conspicuous feature, common to all the radical ion fragmentations studied, is that only one electron configuration stands out at all C–X bond distances. This trait (common to the C and Si systems) puts “mesolysis” in sharp contrast with homolysis. The latter is in fact characterized by the dominance of two-electron configurations along the dissociation pathway. Mesolysis is also divergent from heterolysis in that the one-electron configuration nature of  $\Psi$  is attributed to the spin coupling of one of the two electrons pertaining to the cleaved bond with the originally unpaired electron. The apparent ambiguity of this cleavage process and the peculiarity just

(47) The reaction energies are larger at the CCSD(T) level than at the CAS-MCSCF level. This is attributable to dynamic electron correlation effects, which bring about a larger stabilization of the reactant with respect to the separated products in all cases. In fact, the CAS-MCSCF energy profiles present larger barriers for the reverse processes, and so give more importance to the avoided crossing factor. In the discussion, not much emphasis was put on the comparison of the two sets of data, because the CCSD(T) energy difference estimates are more reliable (see the Methods section). In this study the MCSCF calculations have been instrumental in examining the features of the wave function and generating the geometries for the energy plots.

described further justify the introduction of the word “mesolysis”, which was originally proposed by Maslak<sup>10a</sup> for this kind of dissociative process, on the basis that it presents a mechanistic duality (as dissociation may be formally viewed as homolytic or heterolytic depending on the sharing of the electrons between the two resulting fragments).

In the radical cations, the carbon and silicon systems show the same fragmentation mode, and require similar energies. However, the silyl group is more inclined to accommodate an electric charge than methyl, and this becomes especially important for the negative charge. This feature allows easier dissociations for the anionic silyl systems, in which silide is generated.<sup>48</sup>

**Acknowledgment.** Financial support was provided in part by the Italian MURST through the “Cofinanziamento di Programmi di Ricerca di Rilevante Interesse Nazionale”, within the project “Chimica in Fase Gassosa di Specie Reattive Neutre e Cariche”.

**Supporting Information Available:** A listing of the geometries of the CAS-MCSCF critical points with total CAS-MCSCF and CCSD(T) energies; total energies of the points used for the energy plots. This material is available free of charge via the Internet at <http://pubs.acs.org>.

JO0343681

(48) Silide is easily formed ( $\text{SiH}_4 + \text{NH}_2^-$ ), and the gas-phase acidity of  $\text{SiH}_4$  is ca. 371 kcal mol<sup>-1</sup>, close to those of MeCN and t-BuOH (ref 43b, p 450).